ISSN 0016-7029, Geochemistry International, 2007, Vol. 45, No. 3, pp. 247–260. © Pleiades Publishing, Ltd., 2007.
Original Russian Text © V.V. Knauf, O.V. Knauf, E.G. Skvortsov, E.V. Sharkov, A.V. Chistyakov, 2007, published in Geokhimiya, 2007, No. 3, pp. 282–296.

Unusual PGE Distribution in the Mafic–Ultramafic Rocks of the Early Paleoproterozoic (2.5–2.35 Ga) Drusite (Coronite) Complex of the Belomorian Region, Northern Karelia, Russia

V. V. Knauf[a], O. V. Knauf[a], E. G. Skvortsov[b], E. V. Sharkov[c], and A. V. Chistyakov[c]

[a] *NATI Research Joint Stock Company, ul. Otechestvennaya 3-3a, St. Petersburg, 195030 Russia*
e-mail: natires@natires.com
[b] *FIP-2 Joint Stock Company, ul. Marata 78, St. Petersburg, 191025 Russia*
e-mail: fip2@mail.ru
[c] *Institute of the Geology of Ore Deposits, Petrography, Mineralogy, and Geochemistry, Russian Academy of Sciences, Staromonetnyi per. 35, Moscow, 119017 Russia*
e-mail: sharkov@igem.ru

Received June 9, 2005

Abstract—The PGE pattern and PGM was studied in the rocks of numerous small mafic–ultramafic intrusions of the Early Paleoproterozoic (2.46–2.35 Ga) drusite complex of the Belomorian mobile belt, eastern Baltic Shield, Russia. The chondrite-normalized PGE pattern in the studied rocks (gabbronorites, pyroxenites, and plagioclase lherzolites) is similar to that of the primitive mantle, regardless of the composition of these rocks. It was shown for the first time that different rock types of the drusite complex contain minerals of all six PGE, which makes these rocks principally different from the coeval large layered mafic–ultramafic intrusions with Pd–Pt mineralization at the adjacent Kola and Karelian cratons. This is presumably related to the generation conditions of the parental magmas of the siliceous high-magnesian series (SHMS) and to the practically complete absence of differentiation during the emplacement of the intrusions. Owing to this, the drusite intrusions retained the primary PGE distribution, which is presumably typical of the parental melts of SHMS and was only partially modified by allochemical metamorphism.

DOI: 10.1134/S0016702907030044

INTRODUCTION

It is known that large mafic–ultramafic layered intrusions (Bushveld, Stillwater, and others) located at Precambrian shields are a major PGE source. Analogous large-layered massifs are widespread in the eastern Baltic Shield, where they form, together with gabbronorite dike swarms and volcanic covers, the large igneous Baltic province, occupying practically all the area [1–3]. All of these rocks were derivatives of the unusual Early Paleoproterozoic (2.5–2.3 Ga)siliceous high-magnesian series (SHMS), whose rocks are similar to the Phanerozoic boninite series in major and trace-element composition, mineral chemistry, and in the presence of andesite–dacite volcanic glass, which was found in the weakly altered lavas of the Vetreny Belt riftogenic structure in southeastern Karelia [2, 4].

SHMS differ from the boninite series in having lower ϵNd(T) values varying from –1 to –2, which indicates their origin through large-scale assimilation of lower crust material by the high-temperature mantle magmas [1, 4]. Moreover, these series were formed in different tectonic settings: Phanerozoic boninites are related to island arcs, whereas their Early Paleoproterozoic analogues were formed in within-late settings.

An inherent feature of the Baltic province of SHMS is very unusual dispersed intrusive magmatism that produced numerous small mafic and ultramafic bodies in the Belomorian and Tersk–Lotta mobile zones, which are located along the boundaries of the stable Kola and Karelian cratons with the simultaneously evolved Lapland–Umba Belt.

The Early Paleoproterozoic drusite (coronite) complex of the Belomorian Region is a classic example of this kind of magmatism [5]. It consists of small rootless bodies from a few hundred square meters to, occasionally, a few of square kilometers in size, which were formed during the tectonic flow of the host Archean gneisses and migmatites. They rarely preserve original intrusive relations with the host rocks, generally having tectonic contacts associated with amphibolite-facies reworking and transformation in different amphibolites. In the relatively fresh rocks of the inner parts of the bodies, the metamorphic coronas (drusites) consisting of predominant green hornblende and garnet are formed along grain boundaries.

The rocks that compose these intrusions are compositionally close to cumulates in coeval large layered intrusions at the adjacent cratons (Monchegorsk, Lukkulaisvaara, Burakovskii, and others). Two major rock types are distinguished there: (1) melanocratic peridotites (mainly plagioclase lherzolites), pyroxenites (bronzitites and websterites), and norites; and (2) leucocratic gabbronorites and anorthosites. However, unlike large intrusions in which these rocks form layered series, each drusite body is typically composed of a single rock type, with corresponding composition of the chill zones.

The formation of this complex was a multistage process, which lasted, according to isotope–geochronological datings, for 100 Ma (from 2.46 to 2.36 Ga) with no significant evolution in the rock composition [5]. Deformations that occurred in the Belomorian mobile belt at that time caused variable reworking of these bodies.

A surprising similarity in composition of large PGE-bearing layered intrusions and drusites suggests that the latter might host economic PGE deposits, as is the case with the Canadian shield, where the large PGE–Cu–Ni sulfide deposit was found among the Voiseys Bay's mafic-ultramafic intrusion of similar size [6].

In the Baltic Shield, similar deposits are as yet unknown, and the problem of PGE potential of these intrusions is poorly studied. However, scanty data report the presence of elevated PGE contents in some drusite massifs [7]. Therefore, a special petrological–mineralogical study was carried out on the mafic–ultramafic intrusions of the North Karelia drusite complex to discover PGE mineralization and to specify their ore potential. Results of these works are reported below.

BRIEF GEOLOGIC AND PETROGRAPHIC CHARACTERISTICS OF THE MASSIFS

Samples were taken from six mafic–ultramafic intrusions located in the Zelenoborskii (Bol'shoi Petik Island, Krivoozerskii, and Tolstik Peninsula) and Nil'mozero (Chernaya Rechka, Mount Panfilov, and Nil'mozero) areas (Fig. 1). All massifs are small (about 1–2 km^2 in area) irregularly rounded bodies with faulted contacts with the host Archean granite gneisses and migmatites of tonalite composition. Three of them (Bol'shoi Petik Island, Krivoozerskii, and Chernaya Rechka) consist of juxtaposed older gabbronorites of higher metamorphic grades and less altered, practically unmetamorphosed plagioclase lherzolites. The Nil'mozero and Chernaya Rechka massifs are made up mainly of fresh plagioclase lherzolites and olivine gabbronorites, which were locally affected by metasomatism with the formation of tabular edenite amphibole. The Mount Panfilov Massif consists of strongly altered gabbronorites and gabbronorite anorthosites. Since our efforts were aimed at studying the PGE mineralization in the massifs of different composition, no detailed geological study of the massifs was conducted, but the petrography of samples taken from different parts of the massifs, mainly along its vertical section, was considered in detail.

Petrography

All studied rocks show variably preserved primary magmatic cumulative textures. All peridotites formally (presence of olivine, two pyroxenes, and plagioclase) are attributed to plagioclase lherzolites but are subdivided into three cumulate types on the basis of texture. The following mineral abbreviations will be used in the text: *Ol* olivine, *Opx* orthopyroxene, *Cpx* clinopyroxene, *Pl* plagiolcase, *Crt* chromite, *Mag* magnetite, *Sulf* sulfide, *Bt* biotite, *Hbl* hornblende, and *Gr* garnet.

Plagioclase lherzolites were found in the Krivoozerskii and Chernaya Rechka intrusives. As was mentioned above, this rock includes three cumulates, *Ol* + *Crt*, *Ol* + *Opx* + *Crt*, and *Ol* + *Opx* + *Cpx* + *Crt*, with significant amounts of interstitial plagioclase and clinopyroxene for two former assemblages. These rocks are typically fresh, weakly serpentinized along fissures, with excellently preserved primary magmatic textures and minerals. A concentrically zoned reaction rim with columnar *Opx* in the central part and small *Cpx* with green spinel inclusions in the margin is formed along olivine and pyroxene boundaries. Plagioclase is typically turbid due to inclusion of spinel dust.

The composition of rock-forming minerals was determined on an X-ray microprobe equipped with an EDS spectrometer (ABT-55 Akashi Beam technology, Link 1000). The results are shown in Tables 1–4 and Figs. 2–4.

As is seen in Table 1, ultramafic cumulates contain high-Mg olivine varying from Fo_{78} to Fo_{86} at an average of Fo_{83}. Its composition shows wide variations from Fo_{80} to Fo_{86} even within one sample (sample CH-20, *Ol* + *Opx* + *Crt* cumulate from the Chernaya Rechka intrusive).

Cumulative orthopyroxene (Table 2 and Fig. 2) also has high-Mg composition of $En_{82–83}$. Interstitial *Opx* in *Ol* + *Cpx* cumulate (sample 506) has the lower Mg composition varying from En_{77} to En_{81}. Interstitial clinopyroxene also shows wide compositional variations from pigeonite–augite (subcalcic augite) $Wo_{29}En_{61}Fs_{10}$ to augite $Wo_{40}En_{51}Fs_9$. Such a compositional scatter can be observed even within a single thin section (Table 2, sample CH-20); there is no distinct zoning, though clinopyroxene in places demonstrates complex intergrowths.

Chromites also show wide variations, even within a single thin section (Table 3, sample CH-20). As is seen in Fig. 4, they have low Fe^{3+} content at variable Cr and Al. The highest Al and the lowest Cr contents were found in sample D-503 (*Ol* + *Opx* + *Crt* cumulates). Interstitial plagioclase was studied only in sample CH-20 and corresponds to An_{44}.

These compositional variations are typical of other ultramafic rocks of the Belomorian drusite complex [2].

Pyroxenites (orthopyroxene cumulates) occur only in the Nil'mozero Massif. The cumulus phase is orthopyroxene (bronzite $Wo_5En_{77}Fs_{18}$). Olivine (Fo_{80})

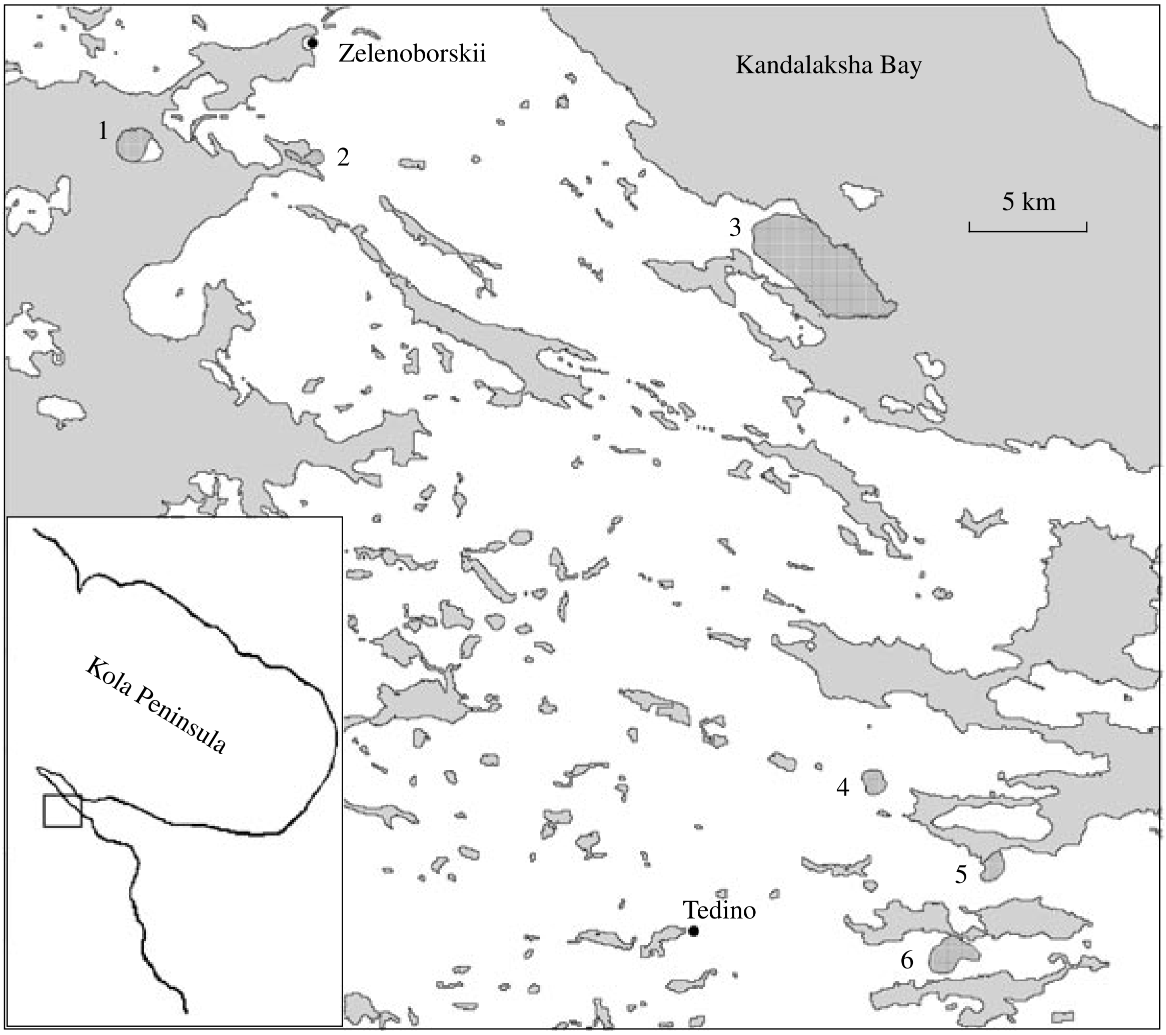

Fig. 1. Position of the studied massifs: (1) Bol'shoi Petik Island; (2) Krivoozerskii; (3) Tolstik Peninsula; (4) Chernaya Rechka; (5) Mount Panfilov; and (6) Nil'mozero.

occurs only as small relics in pyroxenes. Interstitial clinopyroxene is pervasively replaced by bronzite. Like in previous cases, it strongly varies in composition from $Wo_{39.1}En_{56.1}Fs_{4.9}$ to $Wo_{36}En_{55}Fs_{9}$. The rock occasionally contains ferrous chromite.

Olivine gabbronorites and gabbronorites (plagioclase–pyroxene ± olivine cumulates) are observed in the Bol'shoi Petik Island, Nil'mozero, Chernaya Rechka, Tolstik Peninsula, and Mount Panfilova intrusives. As compared to the aforementioned rocks, they were often affected by deformations and overprinted metamorphism with the formation of garnet and garnet–hornblende rims (coronas).

Olivine gabbronorites and gabbronorites occur in the Nil'mozero and Chernaya Rechka massifs. These are fresh rocks with cumulus olivine $Fo_{75–78}$, orthopyroxene $Wo_{3–5}En_{79–88}Fs_{10–16}$, and plagiolcase An_{49}. Their clinopyroxene is particularly interesting, because it often shows oscillatory zoning, grading from pigeonite $Wo_{9–12}En_{70–72}Fs_{18–20}$ in the cores to pigeonite–augite $Wo_{37–41}En_{49–51}Fs_{10–11}$ in the rims (Table 2, Fig. 3), and even from orthopyroxene $Wo_3En_{88}Fs_9$ in the core to pigeonite–augite $Wo_{38}En_{55}Fs_7$ in the rim.

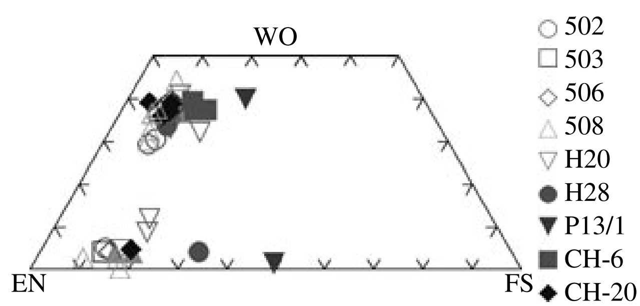

Fig. 2. Composition of pyroxenes from studied drusite bodies plotted on the pyroxene projection.

Table 1. Composition of olivine in the rocks of drusite complex

Sample No.	SiO_2	FeO	MnO	MgO	NiO
CH-6	38.91	20.23	0.32	39.82	0.89
CH-20	39.44	18.29	0.19	42.25	–
CH-20	39.38	18.2	–	42.55	–
CH-20	40.51	13.13	–	46.51	–
504	39.91	15.97	–	44.27	–
504	40.64	16.42	0.28	44.57	–
506	39.1	20.5	–	40.57	–
H-20	38.56	23.26	–	38.35	–
H-28	39.53	18.91	0.23	41.55	–
503	40.15	15.08	–	44.94	–

Note: Dashes mean not determined. Hereinafter: *Krivoozerskii intrusion*: (502) biotitized garnetized gabbronorite (*Cpx–Opx–Pl* cumulate) with zoned partially saussuritized plagioclase; (503) fresh plagioclase lherzolite (*Ol–Opx–Crt* cumulate); interstitial minerals are *Cpx* and *Pl*; (504) fresh plagioclase poikilitic harzburgite (*Ol–Crt* cumulate); interstitial minerals are *Opx*, *Cpx, Pl*; (506) plagioclase poikilitic harzburgite (*Ol–Crt* cumulate). *Bol'shoi Petik Island intrusion*: (508) weakly metamorphosed coarse-grained olivine gabbronorite (*Ol–Pl* cumulate) with *Crt*; intercumulus consists of inverted pigeonite and pigeonite–augite; metamorphogenic coronal textures developed along grain boundaries. *Chernaya Rechka intrusion*: (CH-6) metamorphosed *Ol* norite (*Ol–Opx–Pl* cumulate); (CH-20) fresh *Pl* lherzolite (*Ol–Opx–Crt* cumulate), interstices are filled with *Cpx, Pl*, and *Bt. Nil'mozero Intrusion*: (H-20) fresh olivine gabbronorite (*Ol–Opx–Pl–Crt* cumulate); plagioclase and orthopyroxene are zoned (see text); (H-28) *Ol* fresh bronzitite (*Ol–Opx–Crt* cumulate). *Mount Panfilov Massif*: (P-13/1) gabbroamphibolite with *Opx* and *Cpx* relics and with primary *Pl*; *Cpx* is pale green, cellular, possibly metamorphic; minor amounts of sulfides.

Metamorphosed biotitized gabbronorite (*Opx* + *Cpx* + *Pl* cumulate) with garnet–hornblende coronae (sample K-508) was found at Bol'shoi Petik Island. It contains hypersthene $Wo_4En_{64}Fs_{32}$, pigeonite augite $Wo_{34}En_{55}Fs_{11}$, and labradorite $An_{56–59}$ (Table 4, Fig. 4). Accessory chromite in this rock has the highest-Cr concentration.

Metamorphosed *Mag*-bearing gabbronorite–diorite was found at the Tolstik Peninsula. Garnet–hornblende aggregates form a corona texture. Clinopyroxene corresponds to augite $Wo_{37–39}En_{45–48}Fs_{13–17}$, while plagiolcase has an andesine composition An_{34}. Ore mineral is magnetite.

Gabbroamphibolites after gabbronorites and gabbroanorthosites with pyroxene and biotite relics form the Mount Panfilov body. The preserved pyroxenes have the Fe-richest composition: $Wo_1En_{50}Fs_{49}$ for *Opx* and $Wo_{40}En_{36}Fs_{24}$ for clinopyroxene; plagioclase, andesine $An_{12–28}$, is likely secondary. The major rock-forming minerals are green metamorphic hornblende and plagioclase. The rocks contain Cl-apatite. It should be noted that all hydroxyl-bearing minerals contain Cl, which presumably was a component of the metamorphic fluid.

The chemical compositions of the rocks are presented in table 5, and their REE contents are shown in Table 6. As is seen in Table 6, the strongly metamorphosed mafic rocks differ from fresh varieties in having higher LREE contents at a similar shape of the REE patterns (Fig. 5), attesting to allochemical metamorphism. The most complex REE distribution was obtained from unaltered ultramafic rocks from the Krivoozerskii body (samples 503 and 506). For reasons unknown as of yet, their patterns are similar to those of mafic rocks in contents of LREE, Tb, Dy, and Lu but show unsystematic negative Eu, Gd, Ho, and Yb anomalies.

Thus, in terms of petrographic and geochemical features, the studied intrusives are close to the previously described Belomorian drusites [5]. However, rocks from our collection are remarkably fresh, being affected, at most, only by insignificant metamorphism (if any) and hence, demonstrate primary, unaltered PGE contents. The clinopyroxenes show oscillatory zoning, all minerals widely vary in composition within a single thin section, and pyroxene lamellae typical of large intrusives are absent; all of these features indicating that the massifs were initially small bodies which rapidly solidified in a relatively cold environment with very limited interaction with host rocks. Under such conditions, the rocks preserved their initial PGE distribution, which formed during the crystallization of the melt and did not change up to the present.

PGE MINERALS AND PLATINOID CONTENTS IN THE ROCKS OF THE DRUSITE COMPLEX

Methods. Two types of samples were collected during our fieldwork to analyze for PGM: (1) loose deposits that overlay drusite bodies and, given landscape specifics, can be reliably assigned to bedrock outcrops, and (2) hand specimens from exposed bedrocks. It is worthwhile to collect loose deposits (eluvial, talus, and colluvial), because they typically accumulate fine PGM grains, which were released from bedrocks owing to "natural crushing" during erosion. This significantly increases the mineralogical sensitivity of subsequent PGM study: up to $n \times 0.0001$ g/t in phase concentration equivalent. The metrology and high-sensitivity technique of mineralogical works on PGM "ppm-mineralogy" are described in detail on *www.natires.com.*

PGM finds in loose samples were verified by hand specimens from bedrocks (Table 7), with mineralogical sensitivity on PGM about 0.01 g/t in the phase equivalent of concentration. With rare exceptions, mineralogical data on loose samples were in good agreement with the results yielded by hand specimens.

Main results. We have established mineral modes of occurrence for all six PGE: refractory (Ru, Os, and Ir) PGE and Rh in variable proportions occur in sulfoars-

Table 2. Representative microprobe analyses of pyroxene in the studied rocks of the drusite complex

Sample	SiO_2	TiO_2	Al_2O_3	FeO	Cr_2O_3	MnO	MgO	CaO	Na_2O	Total	WO	EN	FS
CH-6-Opx	154.53	–	2.43	10.58	0.57	–	28.91	1.29	1.32	99.63	2.6	80.8	16.6
CH-6-Cpx1	55.23	–	3.16	3.79	0.85	–	18.51	16.60	1.86	100.00	36.6	56.8	6.5
CH-6-Cpx2c	54.16	0.33	4.65	4.55	0.81	–	18.94	14.46	2.02	99.92	32.6	59.4	8.0
CH-6-Cpx2r	54.55	0.45	5.44	3.54	–	–	12.57	16.17	2.02	94.74	44.4	48.0	7.6
CH-6-Opx2c	56.52	–	1.97	6.23	0.69	–	32.25	1.43	0.81	99.90	2.8	87.7	9.5
CH-6-Opx2mid	55.28	–	3.86	5.20	1.74	–	19.94	13.69	1.48	101.19	30.1	61.0	8.9
CH-6-Opx2r-3	56.20	–	3.50	3.88	–	–	17.61	16.74	2.19	100.12	37.8	55.3	6.8
CH-20-Cpx1	52.69	0.25	3.82	6.15	1.28	–	19.82	14.13	1.54	99.68	30.4	59.3	10.3
CH-20-Cpx2	52.15	0.43	4.63	5.01	1.26	–	17.23	17.23	1.75	99.69	38.2	53.1	8.7
CH-20-Cpx3	54.38	–	2.57	5.77	1.02	–	21.00	14.01	1.15	99.90	29.4	61.2	9.4
CH-20-Cpx4	51.92	0.28	3.53	6.11	1.28	0.19	19.06	16.56	1.62	100.55	34.5	55.3	10.2
CH-20-Opx	55.17	–	2.04	8.47	0.76	–	30.15	2.54	0.86	99.99	5.0	82.1	12.9
503-Cpx	52.37	0.42	3.06	4.68	1.08	–	18.61	17.40	1.57	99.19	37.1	55.2	7.8
503-Opx	55.73	–	1.76	8.30	0.61	–	30.44	2.04	0.88	99.76	4.0	83.3	12.7
504-Cpx	52.45	0.73	3.07	4.91	0.96	0.22	16.85	18.12	1.92	99.23	39.8	51.4	8.8
504-Opx	56.30	0.18	1.38	9.08	0.47	0.27	30.41	2.09	–	100.18	4.0	81.8	14.1
506-Cpx	52.30	0.25	2.95	7.70	1.01	–	18.04	18.19	1.35	101.79	36.9	50.9	12.2
506-Opx1	54.24	–	2.09	11.75	–	0.49	27.98	1.96	2.75	101.26	3.9	77.2	18.9
506-Opx2	55.32	–	1.51	9.91	–	0.21	29.86	2.04	0.84	99.69	4.0	80.7	15.3
508-Cpx1	52.43	0.25	2.57	7.64	0.99	–	21.41	18.06	1.39	104.74	33.6	55.4	11.1
508-Opx2	52.41	–	1.44	22.47	0.61	–	24.87	2.25	1.08	105.13	4.1	63.6	32.2
515-Cpx2	54.78	0.25	2.44	8.31	–	–	14.82	16.17	2.20	98.97	37.4	47.6	15.0
515-Cpx3	54.70	0.22	3.27	9.53	–	–	14.04	16.04	2.27	100.07	37.3	45.4	17.3
515-Cpx4	55.51	–	2.72	7.43	–	–	14.87	17.32	2.21	100.06	39.5	47.2	13.2
H-20-Cpx1	52.90	–	2.44	6.77	0.79	–	17.93	18.03	0.89	99.75	37.4	51.7	10.9
H-20-Cpx2c	48.83	0.25	2.70	11.48	1.04	–	17.23	15.61	1.30	98.44	32.2	49.4	18.5
H-20-Cpx2r	52.43	–	2.25	5.95	0.56	0.22	16.95	19.66	1.44	99.46	40.9	49.1	10.0
H-20-Opx1c	54.74	–	1.40	10.75	0.40	–	29.25	2.38	0.73	99.65	4.6	79.1	16.3
H-20-Opx1mid-2	51.51	0.25	2.78	7.24	1.12	–	18.56	15.48	1.19	98.13	33.0	55.0	12.0
H-20-Opx1r-3	52.24	0.29	3.04	6.62	0.18	0.22	17.63	17.91	1.15	99.28	37.5	51.3	11.2
H-20-Opx2r	52.37	–	1.89	11.73	0.86	0.26	25.43	6.06	0.80	99.40	11.9	69.6	18.4
H-20-Opx2c	53.82	0.15	1.81	12.33	0.45	0.19	25.73	4.37	0.85	99.70	8.8	71.7	19.6
H-28-Cpx3	52.17	0.25	2.68	5.52	1.11	–	19.01	17.23	1.46	99.43	35.9	55.1	9.0
H-28-Opx3c	53.50	–	2.61	11.42	0.70	0.34	28.15	2.38	0.58	99.68	4.7	77.2	18.1
P-4-Cpx	51.27	–	1.54	13.52	–	0.27	11.64	18.03	2.67	98.94	40.1	36.0	23.9
P-4-Opx	51.32	–	–	29.82	–	0.74	17.40	0.73	–	100.01	1.5	49.6	48.9

Note: (c) Core, (mid) intermediate zone, (r) rim.

Table 3. Composition of Cr-spinel

Oxides	CH-6	CH-20-1	CH-20-2	CH-20-3	504-1	504-2	H-515	H-28	508	503
TiO_2	0.60	0.55	0.63	0.60	0.44	0.48	0.00	0.47	0.00	0.30
Al_2O_3	17.46	17.82	21.59	25.72	25.12	26.63	0.87	14.59	13.87	31.20
Cr_2O_3	46.68	43.67	41.43	38.12	35.50	34.85	0.38	34.85	49.79	33.33
Fe_2O_3	2.61	5.53	5.28	4.03	6.11	6.35	67.63	19.85	3.75	2.70
FeO	27.71	26.26	21.91	21.65	25.57	25.87	31.22	8.79	29.06	23.19
MnO	0.00	0.81	0.00	0.37	0.66	0.67	0.00	0.35	0.55	0.43
MgO	5.00	5.38	9.20	9.54	6.61	6.96	0.00	4.10	3.02	8.90
CaO	0.00	0.00	0.00	0.00	0.00	0.00	0.00	15.67	0.00	0.00
Total	100.06	100.02	100.04	100.04	100.01	101.81	100.11	98.68	100.04	100.05
Al	0.68	0.69	0.81	0.94	0.94	0.97	0.04	0.57	0.56	1.12
Cr	1.22	1.14	1.04	0.94	0.89	0.86	0.01	0.91	1.35	0.80
Fe^{+3}	0.07	0.14	0.13	0.09	0.15	0.15	1.95	0.49	0.10	0.06

Note: Compositions are calculated on the basis of 4 oxygens.

enides (ruarsite, platarsite, and hollingworthite), Pt occurs in sulfoarsenides, arsenides, and sulfides (platarsite, sperrylite, and braggite) (Table 9). Pd was found in arsenides and arseno-antimonides (guanglinite, mertieite) and as a minor admixture in sulfoarsenides of refractory PGE, which is very unusual. Major minerals are euhedral sperrylite and sulfoarsenides of Ru, Pt, and Rh (Figs. 6a–e).

Table 4. Microprobe composition of plagioclase in the rocks of drusite complex

Sample	SiO_2	Al_2O_3	CaO	Na_2O	K_2O
CH-6	56.71	27.71	10.08	5.74	no
CH-20	56.56	28.84	8.75	6.05	no
515	57.48	27.71	7.94	8.48	no
H-20	54.78	29.00	9.87	5.60	no
508	53.63	29.54	12.2	4.70	no
508	53.50	29.19	12.8	5.62	no
P-4 (n)	66.00	21.28	2.48	10.15	0.22
P-4 (old)	62.35	24.04	5.80	8.13	no

Note: Sample from the Mount Panfilov body contains two plagioclase: relict magmatic (old) and newly formed (n).

The presence of mineral species of all six PGE in various rock types is a very unusual feature, which differentiates the drusite complex from coeval large layered intrusions of the Baltic Shield having distinctly expressed Pt–Pd specifics. This is also supported by chondrite- and primitive mantle-normalized PGE patterns for major petrographic rock types of the drusite complex shown in Fig. 7. Normalizing values are taken from [8].

PGE DISTRIBUTION IN THE ROCKS OF THE DRUSITE COMPLEX

It can be seen that the distribution patterns of the rocks are similar in shape and contents of noble metals (NM) to the primitive mantle, in spite of the fact that three of them are peridotite cumulates (503, H-4, and CH-20), one is pyroxenite (H-34), and the others are mafic cumulates (508, CH-6). The patterns show small positive Pd anomalies and insignificant negative anomalies of Ir and, especially Os. The exception is sample H-4 (metasoimatized plagioclase lherzolite) with an elevated gold content. The patterns of weakly altered rocks, regardless of their composition, are plotted closely to each other and have similar shapes.

Narrow marginal zones metamorphosed into garnet and biotite amphibolites strongly differ in mineralogy. They contain relatively low-temperature xenomorphous complex bismuthotellurides of Pd and Pt (michenerite, merenskiite, moncheite) but no refractory PGE (Fig. 6f). The same minerals are observed in the narrow outer contact zones of large granite pegmatite bodies cutting across drusite massifs (for example, Mount Panfilov). In addition, metasomatic zones are abundant in elevated contents of Cu and Ni sulfides and contain pyrrhotite, galena, sphalerite, bismuthinite, scheelite, cassiterite, gold, native bismuth, copper, and nickelous iron intergrown with knebelite (Mn-olivine). The presence of these minerals is presumably related to the influx of various components during allochemical metamorphism.

Note that such a PGE distribution was not observed in either ophiolite associations or layered intrusions, and concentrically zoned dunite–clinopyroxenite–gabbro complexes, with different distributions in different rocks of the complexes (Fig. 8). This results in different PGE specialization of rocks from different complexes: Ir–Os–Ru (alpine-type chromitites, and in some cases, chromities at the base of ophiolite layered series); essentially Ir–Pt (concentrically zones complexes), Pt–Pd (in different layered intrusions). The PGE patterns of rocks of drusite complex plot in a narrow range, which is typical of weakly evolved rocks.

The PGE distribution patterns in the studied drusite bodies strongly differ from those of coeval large-layered intrusions in adjacent cratons (Fig. 8). As is seen from this figure, they most closely resemble the patterns of the ore-bearing rocks of the Monchegorsk pluton at the Kola Peninsula and are the most different from that of Lukkulaisvaara PGE-bearing massif in northern Karelia. Mafic cumulates of the Penikat PGE-bearing massif in Finland show intermediate contents of Rh, Pt, and Pd.

The global statistics of PGE abundances in rocks from various complexes indicates that refractory PGE (Ir, Os, Ru) remain in residuum, while Pd–Pt are accumulated in residual melts [9, 10]. C1 chondrite-normalized patterns plotted in order of decreasing melting point in a diagram of refractory PGEs vs. (Pd, Pt) for ophiolite mantle rocks typically show nearly flat distribution (normalized values vary within one order of magnitude], while residuum from this association is enriched in refractory PGE. All layered intrusions exhibit positively sloped pattern, i.e., are enriched in Pt+Pd, with the difference between the normalized contents of refractory and low-melting point PGE (Pd, Pt) reaching a few orders of magnitude (Fig. 8). However, there are some details, for example, the behavior of intermediate Rh, the negative anomaly at Ru, as well as specific patterns in zoned complex, whose nature remains unclear as yet.

As in the rocks of the drusite complex, all six PGEs were found in podiform chromitites of the Kraubath ophiolite massif [11]. However, Pt and Pd occur there in insignificant amounts, presumably indicating that the massif initially contained all PGE, but only refractory PGE remained after depletion. The presence of all PGE in the rocks of the drusite complex likely suggests extremely weak differentiation of primary melt, unlike mantle residuum and direct mantle melts. This is the only exception to the rule, and the reasons for this phenomenon are unclear. The question then arises as to why different rocks, from peridotites to gabbroids, show similar PGE patterns because magmatic differentiation must produce different patterns, which is well illustrated by the example of layered massifs (Fig. 8). In

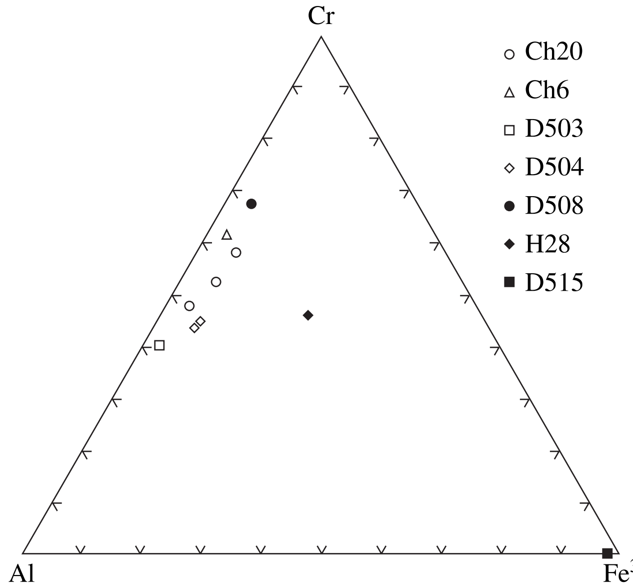

Fig. 3. Composition of Cr-spinel in a Al–Cr–Fe^3 diagram.

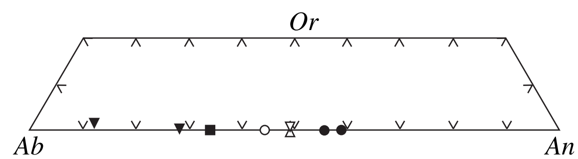

Fig. 4. Composition of plagioclases in the *Ab–An–Or* diagram. Symbols are shown in Fig. 2.

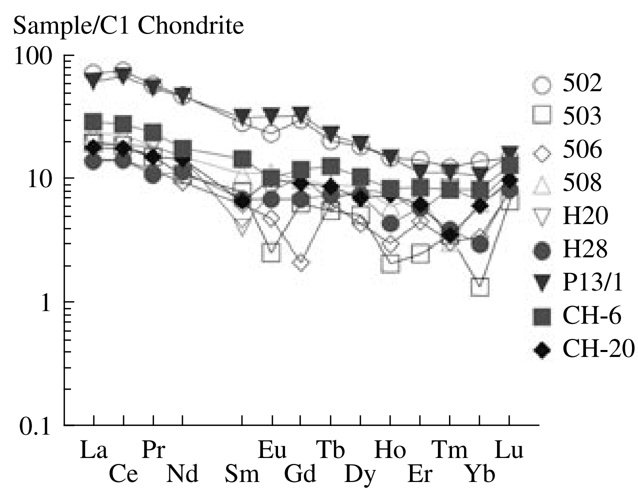

Fig. 5. Chondrite-normalized REE patterns.

Table 5. Chemical analyses of some rocks from the drusite complex

Oxides	502	503	504	506	508	510	H-20	H-28	CH-6	CH-20	P-13/1
SiO_2	53.40	42.30	41.30	46.10	48.80	47.60	44.60	45.40	48.90	44.80	48.90
TiO_2	0.62	0.26	0.16	0.34	0.34	0.23	0.37	0.46	0.49	0.49	2.22
Al_2O_3	15.60	5.00	4.70	8.00	10.80	8.00	7.00	6.50	10.90	7.30	11.80
Fe_2O_3	0.93	3.73	4.62	2.32	1.04	no	0.67	1.98	1.78	1.54	3.74
FeO	5.82	7.35	7.09	9.18	9.41	9.87	8.22	9.92	9.46	9.33	9.95
MnO	0.14	0.20	0.16	0.19	0.17	0.19	0.19	0.19	0.18	0.18	0.18
MgO	7.94	29.06	30.25	23.75	17.38	23.42	25.35	25.72	17.29	26.64	6.66
CaO	9.71	3.54	3.12	7.33	8.75	6.66	11.00	6.05	8.16	6.72	8.86
Na_2O	2.86	0.86	0.78	1.26	1.53	1.19	1.07	1.02	1.51	1.08	4.98
K_2O	1.22	0.35	0.41	0.29	0.39	0.54	0.27	0.22	0.48	0.24	0.96
H_2O^*	0.88	7.09	7.25	0.78	0.71	1.68	0.45	2.19	0.66	0.88	0.91
CO_2	0.24	0.33	0.09	0.41	0.24	0.13	0.30	0.36	0.28	0.26	0.25
P_2O_5	0.26	0.10	0.03	0.10	0.07	0.06	0.05	0.06	0.09	0.09	0.21
Total	99.65	100.17	100.23	100.05	99.63	99.57	99.54	100.07	100.18	99.54	99.62

Note: *Krivoozerskii intrusion*: (502) biotitized garnetized gabbronorite (*Cpx–Opx–Pl* cumulate) with zoned partially saussuritized *Pl*; (503) fresh plagiolcase lherzolite (*Ol–Opx–Crt* cumulate); interstitial minerals are *Cpx* and *Pl*; (504) fresh *Pl* poikilitic harzburgite (*Ol–Crt* cumulate); interstitial minerals are *Opx, Cpx, Pl*; (506) *Pl* poikilitic harzburgite (*Ol–Crt* cumulate). *Bol'shoi Petik Island Intrusion*: (508) weakly metamorphosed coarse-grained *Ol* gabbronorite (*Ol–Pl* cumulate) with *Crt*; intercumulus consists of inverted pigeonite and pigeonite–augite; metamorphic coronae developed along grain boundaries. *Chernaya Rechka Intrusion*: (CH-6) metamorphosed *Ol* norite (*Ol–Opx–Pl* cumulate); (CH-20) fresh *Pl* lherzolite (*Ol–Opx–Crt* cumulate), interstices are filled with *Cpx*, *Pl*, and *Bt*. *Nil'mozero intrusion*: (H-20) fresh olivine gabbronorite (*Ol–Opx–Pl–Crt* cumulate); *Pl* and *Opx* are zoned (see text); (H-28) fresh *Ol* bronzitite (*Ol–Opx–Crt* cumulate). *Mount Panfilov Massif*: (P-13/1) gabbroamphibolite with relict *Opx* and *Cpx*; as well as primary *Pl*; (*Cpx*) pale green cellular likely metamorphic; minor sulfides. Analyses were made by conventional "wet" chemistry at the Institute of the Geology of Ore Deposits, Petrography, Mineralogy, and Geochemistry, Russian Academy of Sciences. $H_2O^* = H_2O^- + H_2O^+$. Analyst Yu.V. Dolinina.

our rocks, this tendency is weakly expressed in the slight positive slope of the PGE patterns.

PGE were redistributed only in the massifs partially metamorphosed to the amphibolite facies and thus transformed into garnet and garnet–biotite amphibolites (for example, the Mount Panfilov Massif). This secondary redistribution has a Pd trend and is evidently related to metasomatic processes that accompanied metamorphism.

DISCUSSION

Studying the PGM and PGE content in the Early Paleoproterozoic drusite complex of the Belomorian Region, we pioneered in establishing that its mafic and ultramafic rocks have the most primitive, possibly mantle PGE patterns, regardless of the rock composition. This fact is inconsistent with currently popular concepts concerning PGE behavior during melting of a mantle source and the subsequent differentiation of the melts in intrusive chambers.

This situation is presumably related to the origin of parental SHMS magmas, whose crystallization produced intrusions of the drusite complex. As was shown earlier, these intrusives are part of the large Baltic igneous province of SHMS related to the activity of an Early Paleoproterozoic mantle superplume [3]. The ultramafic material of this plume, unlike that of Phanerozoic superplumes, was strongly depleted via previous melting events (during the formation of the lobal magmatic ocean and the subsequent Archean evolution of the Earth: [16]) and represent a residuum. The melting

Table 6. Content of REE (ppm) in the rocks of the drusite complex

Elements	502	503	506	508	H-20	H-28	CH-6	CH-20	P-13/1
La	17.07	4.66	3.44	5.56	4.77	3.31	6.88	4.31	14.73
Ce	46.04	11.55	8.77	14.05	11.61	8.84	17.09	10.95	42.02
Pr	5.54	1.45	1.11	1.78	1.77	1.03	2.27	1.44	5.22
Nd	22.23	5.13	4.39	7.11	7.12	5.41	8.42	6.83	22.07
Sm	4.37	1.21	0.95	1.7	0.62	1.05	2.23	1.02	4.81
Eu	1.36	0.15	0.28	0.66	0.46	0.4	0.6	0.58	1.89
Gd	6.26	1.32	0.44	2.02	2.18	1.43	2.45	1.92	6.72
Tb	0.77	0.21	0.24	0.34	0.25	0.28	0.48	0.33	0.87
Dy	4.72	1.3	1.12	2.24	2.15	1.89	2.67	1.78	4.88
Ho	0.85	0.12	0.17	0.34	0.43	0.25	0.48	0.42	0.84
Er	2.39	0.42	0.76	1.25	0.9	0.97	1.43	1.03	1.88
Tm	0.32	0.09	0.08	0.08	0.22	0.1	0.21	0.09	0.29
Yb	2.39	0.23	0.58	1.08	1.14	0.51	1.41	1.04	1.83
Lu	0.38	0.17	0.2	0.23	0.3	0.21	0.33	0.25	0.4

Note: Analyses were conducted at the Central Chemical Laboratory of the Institute of the Geology of Ore Deposits, Petrography, Mineralogy, and Geochemistry, Russian Academy of Sciences, using a PLASMA QUARD PQ2+ TURBO (VG INSTRUMENTS) quadrupole mass spectrometer. Analysts S.A. Gorbacheva, V.D. Sidel'nikova, and L.S. Tsimlyanskaya.

Table 7. Contents of noble metals in the rocks of the drusite complex (ppb)

Sample No.	Au	Ir	Os	Pd	Pt	Rh	Ru	Σ(–Au)
502	0.68	<0.1	<1	1.12	0.75	<1	<2	1.87
503	1.51	1.21	1.04	10.9	10.9	1.91	7.02	32.98
508	1.06	0.67	<1	10.6	10.1	1.47	3.44	26.28
H-4	27.5	1.86	1.39	10.2	9.84	1.82	6.75	31.86
H-34	0.95	1.33	<1	23.2	18.8	3.23	6.21	52.77
CH-6	3.63	0.77	<1	10.4	10.6	1.46	3.59	26.82
CH-20	1.39	2.19	1.43	8.45	9.23	1.49	6.59	29.38

Note: Analyses were performed at the Geolaboratory of the Geological Survey of Finland, Espoo.

of this source must have produced melts enriched in refractory PGEs and depleted in low-melting PGEs. During the subsequent stage, the chambers of these melts ascended (floated) through the Earth crust in compliance with the zoned refinement mechanism, i.e., by the melting of the roof and crystallization near the bottom, being assisted by large-scale crustal assimilation [17].

It was shown earlier that the mafic lower crust of the Belomorian Belt was formed by the underplating of Archean mantle komatiite–basaltic melts and Early Paleoproterozoic SHMS melts, which were emplaced along the mantle–crust boundary [18, 19]. Correspondingly, these lower crustal rocks must be enriched, by contrast, in low-melting PGE. The superposition of these two sources presumably provided the observed pattern. The absence of differences in PGE patterns between the mafic and ultramafic rocks of the complex is presumably also related to the formation mechanism of SHMS magmas. Mafic magmas that formed gab-

Table 8. Chemical composition of PGM shown in Fig. 6

Mineral	Photo	Co	Ni	Cu	Ru	Rh	Pd	Os	Ir	Pt	S	As	Sb	Te	Bi	Total
SPR	a	–	–	–	–	–	–	–	–	55.7	–	44.3	–	–	–	100.0
		–	–	–	–	–	–	–	–	0.977	–	2.023	–	–	–	3.000
Pt-RAS	a	0.7	0.6	–	17.1	2.9	5.3	2.9	0.5	24.8	14.2	30.5	–	–	–	99.5
		0.027	0.021	–	0.403	0.067	0.118	0.036	0.006	0.303	1.050	0.969	–	–	–	3.000
Pd-RAS	a	1.1	0.7	–	17.9	–	11.5	3.8	0.8	17.5	14.4	32.0	–	–	–	99.7
		0.042	0.027	–	0.406	–	0.248	0.045	0.009	0.206	1.033	0.982	–	–	–	3.000
Pt, Ru-HGW	b	–	0.3	–	9.3	16.1	–	–	–	28.2	13.3	32.6	–	–	–	99.8
		–	0.009	–	0.221	0.376	–	–	–	0.348	0.998	1.048	–	–	–	3.000
Pt-HGW	b	–	0.4	–	3.1	31.6	–	–	–	18.0	13.2	33.3	–	–	–	99.6
		–	0.012	–	0.071	0.714	–	–	–	0.214	0.956	1.033	–	–	–	3.000
Rh-PTAS	b	–	0.3	–	7.9	15.1	–	1.9	–	30.3	12.1	31.5	–	–	–	99.1
		–	0.012	–	0.196	0.370	–	0.024	–	0.391	0.950	1.057	–	–	–	3.000
SPR	c	–	–	–	–	–	–	–	–	55.9	–	44.1	–	–	–	100.0
		–	–	–	–	–	–	–	–	0.983	–	2.017	–	–	–	3.000
GU	d	–	–	–	–	–	78.0	–	–	–	–	15.8	5.5	–	–	99.3
		–	–	–	–	–	2.964	–	–	–	–	0.853	0.183	–	–	4.000
ME II	d	–	–	0.9	–	–	72.6	–	–	–	–	9.2	12.9	4.0	–	99.6
		–	–	0.157	–	–	7.865	–	–	–	–	1.404	1.213	0.360	–	11.000
BR	e	–	1.4	–	–	–	5.9	–	–	75.9	16.4	–	–	–	–	99.6
		–	0.046	–	–	–	0.113	–	–	0.796	1.045	–	–	–	–	2.000
MI	f	–	–	–		–	24.7	–	–	–	–	–	–	28.5	46.5	99.7
		–	–	–		–	1.027	–	–	–	–	–	–	0.988	0.985	3.000

Note: The first row in the table denotes concentration (wt %), the second row denotes formula units.

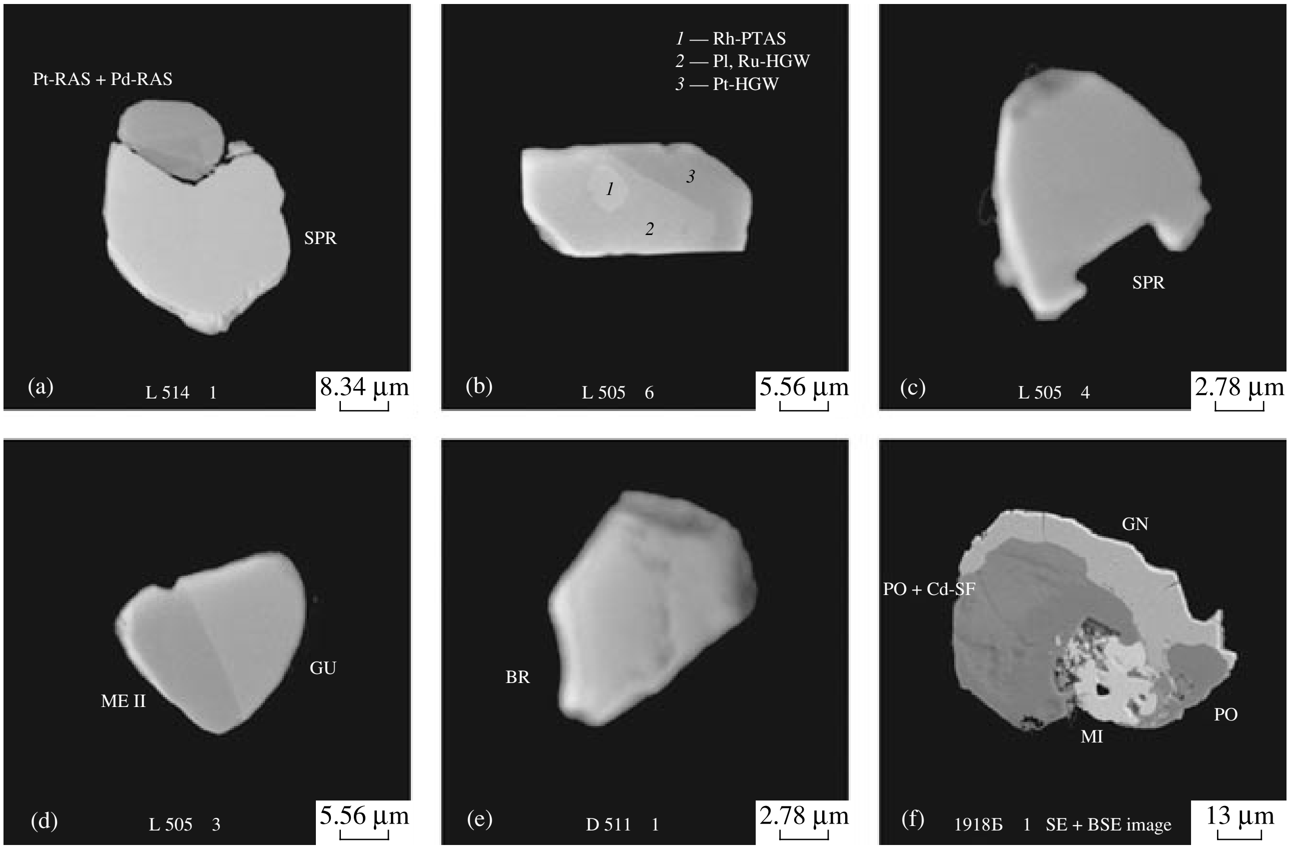

Fig. 6. PGE minerals in the rocks of the drusite complex: (a–e) euhedral PGE minerals in the weakly altered rocks of the complex; (f) assemblage of low-temperature anhedral minerals from metasomatized drusites. Abbreviations: (RAS) ruarsite, RuAsS; (PTAS) platarsite, PtAsS; (HGW) hollingworthite, RhAsS; these sulfoarsenides contain trace Os and Ir. (SPR) sperrylite, $PtAs_2$; (ME) mertieite, $Pd_8(Sb,As)_3$; (GU) guanglinite, Pd_3As; (BR) braggite, (Pd,Ni)S; (MI) michenerite, PdTeBi; (PO) pyrrhotite, FeS; (SF) sphalerite, ZnS; (GN) galena, PbS. Massifs of Bol'shoi Petik Island, Krivoozerskii, Nil'mozero, and Mount Panfilov. Minerals were identified on a scanning electron microscope ABT-55 with EDS LINK 10000.

broids could, in this case, be produced not by crystallization differentiation in the chamber but rather by melts that were derived during lower crustal assimilation and individually emplaced in the Earth's crust, as is typical of the rocks of the drusite complex [5].

The question arises as to why large-layered massifs and small drusite intrusions that were derived from similar melts have different PGE mineralization. The main difference is evidently related to the mechanism of their formation. The layered intrusions of cratons were large crustal intermediate chambers that accumulated melts that periodically were supplied from the magma generation zone into the solidifying intrusive chamber, where they crystallized to produce layering [17]. Owing to this, the PGE distribution pattern was defined mainly by melt differentiation in the plutonic chambers.

However, the mobile conditions of the Belomorian belt prevented the formation of large stable chambers in which crystallization processes operated. The ascending melts could be localized only in small chambers, which were formed at local heterogeneities (folds, detachments, local extensional zones, and others)

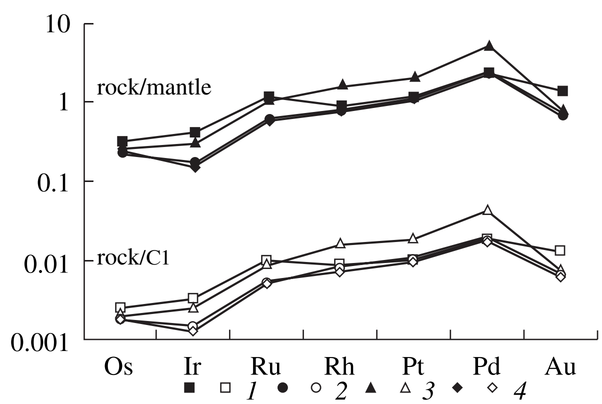

Fig. 7. C1 chondrite- and primitive mantle-normalized PGE patterns for the mafic–ultramafic rocks of the drusite complex. Normalizing values are from [8]. (*1*) plagiolcase lherzolites, (*2*) gabbronorite, (*3*) olivine bronzitites, (*4*) olivine norites.

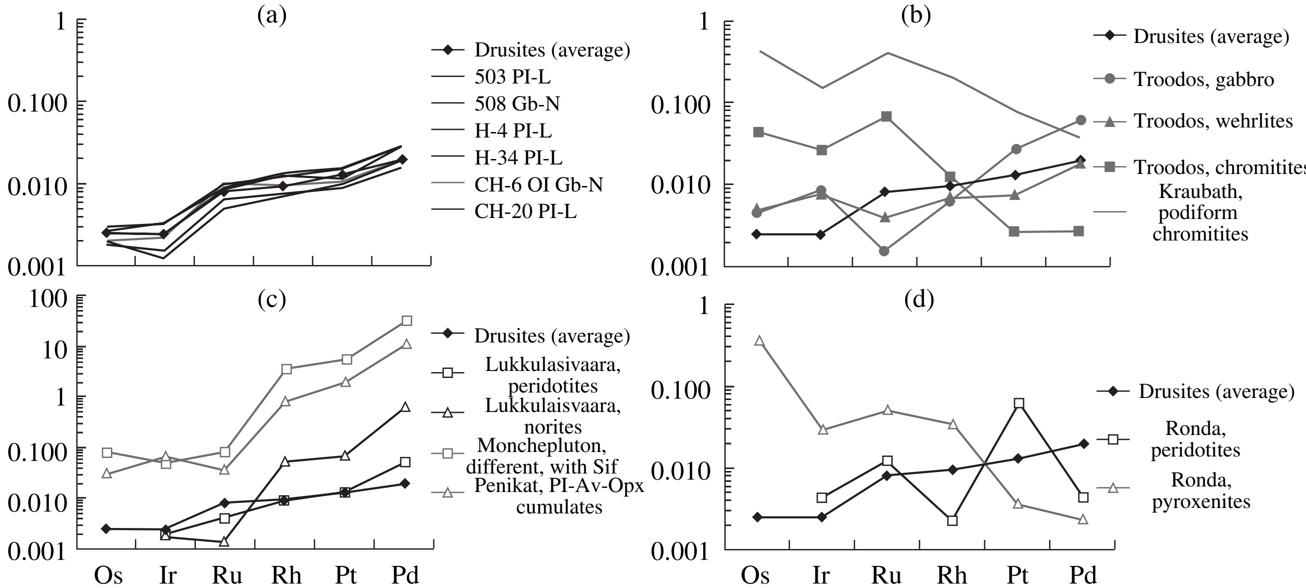

Fig. 8. Comparison of chondrite-normalized PGE patterns in different rocks of the drusite complex of Karelia (a) with those of ophiolite associations [11–13] (b), layered mafic–ultramafic intrusions of the Karelia–Kola area (based on original data and data of T.L. Grokhovskaya, Yu.N. Yakovlev, A.U. Korchagin, and others [14]) (c), and tectonic blocks of mantle in the Gibraltar arc (Ronda and Beni Bouchera massifs [15]) (d).

Table 9. Composition of minerals from some samples

Element	Sample				
	504		508		CH-6
	Bi (1)	PO (7)	Rh,Pt,Ru-GF (1)	NC (2)	PO-MIL? (1-Sulf)
Fe	–	60.4	2.6	–	27.8
Co	–	0.3	6.9	–	1.1
Ni	–	0.3	21.6	45.2	34.1
Ru	–	–	1.3	–	–
Rh	–	–	2.3	–	–
Pt	–	–	3.7	–	–
S	–	38.5	18.4	–	36.6
As	–		42.6	53.9	–
Sb	–	–	–	0.8	–
Bi	99.8	–	–	–	–
Total	99.8	99.5	99.4	99.9	99.6
			Numbers of cations		
Fe	–	0.944	0.079	–	0.445
Co	–	0.004	0.203	–	0.015
Ni	–	0.004	0.640	1.030	0.519
Ru	–	–	0.021	–	–
Rh	–	–	0.038	–	–
Pt	–	–	0.033	–	–
S	–	1.048	0.998	–	1.021
As	–	–	0.989	0.962	–
Sb	–	–	–	0.008	–
Bi	1.000	–	–	–	–
Total	1.000	2.000	3.000	2.000	2.000

Note: Microprobe determinations were made by V.V. Knauf.

repeatedly caused during the tectonic flow of the host rocks. In addition, the chambers periodically migrated, preventing melt accumulation at a single site and, thus, the formation of large bodies. Small bodies solidified rapidly, without significant differentiation, as is confirmed by available geological and petrological data [5]. A slight positive slope in PGE patterns attests to insignificant differentiation, which exerted no effect on the general situation.

In other words, the magmas that formed drusite bodies came directly from the magma generation area and possessed unchanged original characteristics, including the PGE distribution. In this case, the gabbronorites of the drusite complex are not differentiates but were derived by the strong contamination of the mantle melt with the lower crustal mafic material (value of ϵNd(2.45) varies form +0.2 to –1.8 [20]). The drusite complex reflects a unique situation when melts were not affected by crystallization differentiation in an intermediate magmatic chambers, unlike most melts. This facilitated the preservation of the initial PGE distribution, which is presumably typical of primary SHMS melts and was partially changed during superimposed allochemical metamorphism. It is interesting in this context that a similar PGE pattern was observed in the 2.52–2.46-Ga ultramafic lavas described in the Gawler craton, South Australia [12]. They are compositionally similar to the Early Paleoproterozoic boninite-like picrites of the Vetreny Belt riftogenic structure in southeastern Karelia, which belongs to the large Baltic igneous province of SHMS [2].

Thus, our data indicate that SHMS melts were initially enriched in PGE, which explains the presence of

PGE ores in many large layered mafic–ultramafic massifs (Bushveld in South Africa, Stillwater in the United States, Pana–Fedorova Tundra in Russia, and others).

CONCLUSIONS

1. The distribution of PGE and their minerals was studied in the rocks from six intrusives of the Early Paleoproterozoic (2.46–2.35 Ga) drusite complex in northern Karelia. This complex consists of numerous small synkinematic mafic–ultramafic intrusions scattered throughout the Belomorian mobile belt in the eastern Baltic Shield. Like the coeval PGE-bearing layered mafic–ultramafic intrusions of the adjacent Kola and Karelian cratons, drusites were derivatives of siliceous high-magnesian (boninite-like) series (SHMS). However, unlike large-layered massifs, the main rock types of the drusite complex typically form individual intrusions with the corresponding composition of the chill zones.

2. The rocks of the complex contain minerals of all six PGE. Refractory (Ru, Os, and Ir) PGE and Rh in variable proportions occur in the form of sulfoarsenides (ruarsite, platarsite, and hollingworthite), Pt is present in sulfoarsenides, arsenides, and sulfides (platarsite, sperrylite, and braggite), while Pd was found in arsenides and arseno-antimonides (guanglinite, mertieite), and in trace amounts in sulfoarsenides of refractory PGE, which is unusual for this element. The major minerals are euhedral sperrylite crystals and sulfoarsenides of Ru, Pt, and Rh. The presence of minerals of all six PGE makes the drusite complex significantly different from coeval large layered mafic–ultramafic intrusions from the adjacent cratons, which have pronounced Pd–Pt specialization.

3. Notable mineralogical differences are observed in the metamorphosed marginal parts of the bodies, which were partially transformed into garnet and biotite amphibolites. The rocks contain relatively low-temperature anhedral complex bismutotellurides of Pd and Pt (michenerite, merenskiite, and moncheite), while refractory PGE are absent. This secondary redistribution has mainly Pd specifics, being evidently related to metasomatic processes that accompanied regional metamorphism.

4. It was established that the C1-normalized PGE distribution pattern in the rocks of the complex (gabbronorites, pyroxenites, and plagioclase lherzolites) are similar to that of the primitive mantle, regardless of composition. The patterns span a narrow range and show the same proportions as that of C1 chondrite, with a weak positive slope indicating some Pt and Pd enrichment of the rocks.

5. This is supposedly related to the origination of parental SHMS magmas through the large-scale assimilation of the lower crustal mafic material by high-temperature mantle melts and to the almost complete absence of differentiation during the emplacement of drusite intrusions. Because of this, drusite massifs retained the primary PGE distribution typical of the parental SHMS melts and was only partially changed during allochemical metamorphism. In the large layered mafic–ultramafic intrusions that were also produced by SHMS melts, the PGE pattern was determined mainly by within-chamber crystallization differentiation, resulting in a distinct trend.

6. Thus, the example of the drusite complex was used to obtain the first data on the PGE distribution in the primary SHMS melts, which were also parental for large Early Paleoproterozic PGE-bearing layered mafic–ultramafic intrusions.

ACKNOWLEDGMENTS

Field and cameral studies were financially supported by NATI and FIP-2 Joint Stock Companies and supported by the Russian Foundation for Basic Research (project no. 04-05-64581).

REFERENCES

1. E. V. Sharkov, V. F. Smol'kin, and I. S. Krassivskaya, "Early Proterozoic Igneous Province of Siliceous High-Mg Boninite-like Rocks in the Eastern Baltic Shield," Petrologiya **5**, 503–522 (1997) [Petrology **5**, 448–465 (1997)].
2. K. A. Evseeva, I. S. Krassivskaya, A. V. Chistyakov, and E. V. Sharkov, "Early Proterozoic Boninite-Like Volcanic Rocks of Vetrny Belt, Eastern Baltic Shield, Russia" Litosfera, No. 3, 110–126 (2004).
3. E. V. Sharkov, K. A. Evseeva, I. S. Krassivskaya, and A. V. Chistyakov, "Magmatic Systems of the Early Paleoproterozoic Large Baltic Igneous Province of Siliceous High-Magnesian (Boninite-like) Series," Geol. Geofiz., No. 9, 968–980 (2005).
4. *Boninites*, Ed. by A. J. Crawford, (Unwin Hyman, London, 1988).
5. E. V. Sharkov, I. S. Krasivskaya, and A. V. Chistyakov, "Dispersed Mafic–Ultramafic Intrusive Magmatism in Early Paleoproterozoic Mobile Zones of the Baltic Shield: An Example of the Belomorian Drusite (Coronite) Complex," Petrologiya **12**, 632–655 (2004) [Petrology **12**, 561–582 (2004)].
6. A. J. Naldrett, *Magmatic Sulfide Deposits of the Copper–Nickel and PGE Ores* (SPbGU, St. Petersburg, 2003) [in Russian].
7. F. P. Mitrofanov, M. M. Efimov, and M. N. Bogdanova, "Lherzolite–Gabbronorite Complex of Belomorides: Geology, Affiliation, and Potential PGE Content," in *Russia's Platinum*, Vol. 2, Book 2, pp. 42–50 (1995) [in Russian].
8. W. F. McDonough and S. Sun, "The Composition of the Earth," Chem. Geol. **120**, 223–253 (1995).
9. R. A. Lord, H. M. Prichard, and C. R. Neary, "Magmatic Platinum-Group Element Concentrations and Hydrothermal Upgrading in the Shetland Ophiolite Complex," Trans. Inst. Mining and Metallurgy. Sect. B, Applied Earth Sci. **103**, B87–B106 (1994).

10. A. J. Naldrett, "World-Class Ni–Cu–PGE Deposits: Key Factors in Their Genesis," Miner. Deposita **34** (3), 227–240 (1999).

11. K. N. Malich, O. A. R. Thalhammer, V. V. Knauf, and F. Melcher, "Diversity of Platinum-Group Mineral Assemblages in Banded and Podiform Chromitite from the Kraubath Ultramafic Massif, Austria: Evidence for An Ophiolitic Transitional Zone?," Mineral Deposita **38**, 282–297 (2003).

12. D. M. Hoatson, S.-S. Sun, M. B. Duggan, et al., "Late Archean Lake Harris Komatiite, Central Gawler Craton, South Australia: Geologic Setting and Geochemistry," Econ. Geol. **100**, 349–374 (2005).

13. H. M. Prichard and R. A. Lord, "Platinum and Palladium in the Troodos Ophiolite Complex, Cyprus," Can. Mineral. **28**, 607–617 (1990).

14. *Geology and Genesis of PGM Deposits*, Ed. by N. P. Laverov and V. V. Distler (Nauka, Moscow, 1994) [in Russian].

15. K. Gueddari, M. Piboule, and J. Amosse, "Differentiation of Platinum-Group Elements (PGE) and of Gold during Partial Melting of Peridotites in the Lherzolitic Massifs of the Betico-Rifean Range (Ronda and Beni Bousera)," Chem. Geol. **134** (1–3), 181–197(1996).

16. O. A. Bogatikov, V. I. Kovalenko, E. V. Sharkov, and V. V. Yarmolyuk, *Magmatism and Geodynamics. Terrestrial Magmatism throughout the Earth's History*, (Gordon–Breach Science, Amsterdam, 2000).

17. E. V. Sharkov, "Layered Intrusions as Transitional Magma Chambers above the Local Plumes of Large Igneous Rock Provinces: Evidence from the Early Paleoproterozoic Province of a Siliceous Highly Magnesian Rock Series in the Baltic Shield," Russ. J. Earth Sci. **5** (4), 1–10 (2003).

18. P. D. Kempton, H. Downes, E. V. Sharkov, et al., "Petrology and Geochemistry of Xenoliths from the Northern Baltic Shield: Evidence for Partial Melting and Metasomatism in the Lower Crust Beneath An Archean Terrane," Lithos **36**, 157–184 (1995).

19. H. Downes, P. Peltonen, I. Manttari, and E. V. Sharkov, "Proterozoic Zircon Ages from Lower Crustal Granulite Xenoliths, Kola Peninsula, Russia: Evidence for Crustal Growth and Reworking," J. Geol. Soc. London, **159**, 485–488 (2002).

20. S. B. Lobach-Zhuchenko, N. A. Arestova, V. P. Chekulaev, et al., "Geochemistry and Petrology of 2.40–2.45 Ga Magmatic Rocks in the North-Western Belomorian Belt, Fennoscandian Shield, Russia," Precambrian Res. **92**, 223–250 (1998).